FROST MEASUREMENT OF AIR SOURCE HEAT PUMP HEAT EXCHANGERS BASED ON IMAGE RECOGNITION PROCESSING TECHNOLOGY

by

Liming CHEN[a] and Bin XIE[b*]

[a] School of Electronic Information and Artificial Intelligence,
Leshan Normal University, Leshan, China
[b] Dean's office of the Engineering and Technical of Chengdu University of Technology,
Leshan, China

Original scientific paper
https://doi.org/10.2298/TSCI2402363C

In order to understand the application of frost measurement of air source heat pump heat exchanger, a research on frost measurement of air source heat pump heat exchanger based on image recognition processing technology is put forward. In this paper, the scheme design of defrosting control system based on image processing technology is introduced, and the frost degree coefficient of outdoor heat exchanger fin surface is introduced to characterize the frost degree of fin surface. Secondly, the experimental environment room was built, and the conventional defrosting control method of the existing heat pump unit was tested on the spot. It was found that in the air temperature of –6~0 °C and the air relative humidity of 86~92%, the unit appeared the phenomenon of "defrosting in time" and "defrosting without frost". Finally, the change of frost layer on the surface of the outdoor heat exchanger fin during defrosting is analyzed, and the coefficient of frost degree on the surface of the fin is calculated and analyzed. At the beginning of defrosting, due to the large degree of frost, the P-value of the frost degree coefficient on the surface of the fin is close to 1, when the defrosting is carried out for 125 seconds, the P-value of the frost degree coefficient on the surface of the fin decreases sharply to 0.09, when the defrosting is completed, the P-value of the frost degree coefficient on the surface of the outdoor heat exchanger is maintained at about 0.04. The defrosting control method of air source heat pump based on image processing technology is proposed in this paper, and its technical feasibility and effect are verified by experimental tests, which lays a foundation for future popularization and application.

Key words: *image recognition, air source, heat pump heat exchanger*

Introduction

Air source heat pump (ASHP), as a renewable energy technology, has become an important form of building energy in China. When ASHP operates in winter, its outdoor heat exchanger will frost, causing a decrease in unit COP, attenuation of heating capacity, and even causing compressor damage and other accidents. Defrosting as needed is necessary to ensure efficient operation of ASHP. However, existing defrosting control methods are difficult to accurately monitor the growth of frost layers, leading to frequent *false defrosting* accidents and seriously affecting the actual operational performance of ASHP. In order to accurately monitor

* Corresponding author, e-mai: BinXie26@126.com

the degree of frost formation in air source heat pumps, existing research has extensively explored indirect and direct frost measurement methods. Among them, the indirect frost measurement method indirectly estimates the degree of frost formation in ASHP units by monitoring changes in factors such as outdoor temperature, relative humidity, and operating time that affect frost formation. The direct frost measurement method directly monitors the degree of frost formation on the surface of the outdoor heat exchanger of the unit through technologies such as laser thickness measurement, micrometer thickness measurement, and photoelectric thickness measurement [1, 2]. Direct frost measurement can more intuitively and accurately monitor frost layer growth compared to indirect frost measurement. However, existing direct frost measurement technologies have the limitations of *point* monitoring and are limited by factors such as operating space and cost, making it difficult to carry out practical engineering applications. When the heat exchanger surface is frosted, its grayscale changes from dark to bright, and the corresponding gray value changes from small to large. Based on the heat exchanger surface image recognition gray, it is conducive to accurate frost measurement. Yan, *et al.* [3] conducted a preliminary exploration on image recognition frost measurement, and experimentally verified the feasibility of the principle of image recognition frost measurement. Image recognition frost detection technology has advantages such as sensitivity and low cost, but in practical applications, the continuous changes in outdoor lighting environment can cause changes in image grayscale recognition, thereby affecting the accuracy of frost detection. Rangayya *et al.* [4] established a transient model of an air source heat pump unit using the hot air defrosting method. The model predicts defrosting time and the distribution of latent and sensible heat energy consumption during defrosting by inputting environmental temperature and humidity, frost thickness, frost density, coil geometry, and bypass hot air temperature. This model proposes for the first time an energy calculation method for thermal convection and wet vapor re evaporation during the defrosting process.

With the deepening of relevant research, a wide variety of defrosting control methods are constantly emerging. However, according to the basic types of defrosting, they can be roughly divided into two types, namely direct measurement based defrosting control methods and indirect measurement based defrosting control methods. The most desired state for defrosting is on-demand defrosting, which starts when defrosting is needed and stops immediately after the frost layer melts. At present, most of the defrosting control methods put into production on the market are temperature time defrosting control, which uses two independent parameters to determine the frost state of outdoor units. This method cannot make accurate judgments and can easily lead to the phenomenon of *false defrosting*. Hence, to take care of the aforementioned issues, this study joins picture handling innovation foster another productive and precise thawing out control strategy, which can really tackle the issue of continuous *bogus thawing out* mishaps in air source heat siphons. This technique has the qualities of low thawing out activity energy utilization and high thawing out productivity [5, 6].

Methods

Design of defrosting control system based on image processing technology

The air source heat pump defrosting control system based on image processing technology is based on the frost formation diagram of the outdoor heat exchanger fins of the air source heat pump. The image is processed by a computer to obtain the judgment conditions for the start and end of defrosting. The controller then sends defrosting start and stop commands to the heat pump unit, mainly including the frost generation section of the outdoor heat exchanger fins of the heat pump unit and the frost image acquisition section II, computer software Part III, and signal control Parts I and IV. When the heat pump unit is working, as the heating mode progresses, the fins of the outdoor heat exchanger of the unit will gradually generate a frost layer. The frosting image of the fins is collected in real-time through a CMOS camera and connected to a computer through a data interface. The computer uses Visual Basic software program to process the collected frosting image and obtain the criteria for defrosting start/stop. The signal is transmitted to the unit through a signal controller to achieve defrosting start/stop, fig. 1.

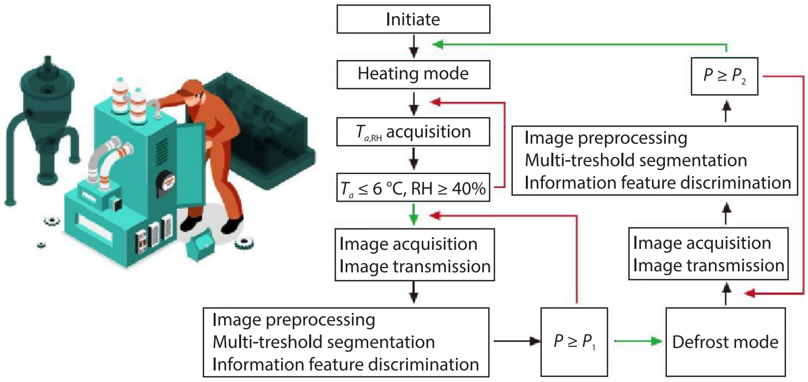

Figure 1. Logic diagram of air source heat pump defrosting control based on image processing technology

Hardware composition of control system

The control system hardware of this study includes image acquisition devices, signal controllers*, etc.*

Image acquisition equipment. With the continuous development of science and technology, sensor technology has also made significant progress, and its application in image processing is becoming increasingly mature. In the 1960's, CMOS image sensors were proposed. With the continuous development of new technologies, they have advantages such as fast data storage and reading speed, high integration, and low cost [7]. The specific structure is shown in fig. 2.

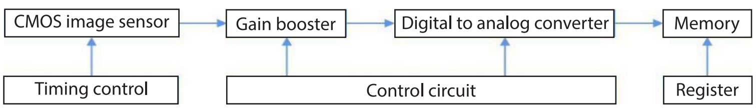

Figure 2. Basic structure of CMOS image sensor

In order to capture real-time images of frost formation on the surface of outdoor heat exchanger fins, the author selected a CMOS camera, model RER-USB500W05G-FV100. This model product is a 1/2.5-inch CMOS camera with the highest effective pixel of 2593(H)×1945(V), which comes with an integrated advanced camera system. The camera can be adjusted 360° left and right to meet the shooting needs of various angles, and can be connected to the computer through the USB2.0 interface to transmit real-time captured images to the computer, preparing for the next step of image digital processing. Table 1 lists the parameters of this type of image sensor, which can meet the author's requirements for collecting frost images on the surface of outdoor heat exchanger fins.

Table 1. The CMOS camera parameters

Product model	RER-USB500W05G-FV100
Output image format	MJPEG
Interface type	USB2.0
Photosensitive film	Magnesium light MI5100 (1/2.5)
Supported resolutions and frame rates	2593×1945 15 fps/2045×1535 16 fps/1620×1210 16 fps/1290×1025 16 fps /1930×1090 302 fps/1270×730 32 fps/820×650 32 fps/650×490 32 fps

Signal controller. Using the VISUAL BASIC program in the computer to program and calculate the information feature discrimination of the image, which is the control signal for defrosting start and stop. The control signal needs to be transmitted to the heat pump unit to control the switching operation of heating and defrosting conditions, which is also an important step in defrosting control. Based on the actual situation of the unit, this experiment uses a DAS air conditioning signal controller, and through the modification of the control panel of the heat pump unit, combined with this signal controller, the control process of the unit's heating and defrosting conditions can be achieved.

Control system software design

In recent years, with the development of computer science, VISUAL BASIC visual programming language has also been rapidly promoted in various industries, including hundreds of statements, keywords, and functions, many of them are closely related to the WINDOWS GUI. The VISUAL BASIC language is simple and easy to learn. It can carry out a lot of interaction design, and has developed the most simple method of platform based application, which has been favored by many programmers, at the same time, its simple operation interface is also easy for non-professionals to master and use. The author used VISUAL BASIC 6.0 language and developed a program based on a computer WINDOWS 7 system, including image acquisition, image preprocessing, image threshold segmentation, and information feature discrimination:

Image preprocessing: The image pre-processing can reduce or remove the interference information on the image by grayscale, smoothing, sharpening, histogram equalization and other methods. For example, the small blockage and other sundries on the surface of the heat exchanger fin can be removed by pre-processing. However, when the interference points are removed from the image, the image contrast will decline, affecting the recognition of the outline of the frosting area, therefore, sharpening and histogram equalization are needed to enhance the frost area contour and local image contrast.

Because the color image processing is to process three color channels at the same time, in order to reduce the calculation pressure of the program and improve the calculation speed, the characteristics of the frost area and non-frost area images are taken into consideration at the same time to realize the conversion of color images to grayscale. In gray-scale digital images, there is only one color channel in each pixel, that is, there is only brightness information but no color information in grayscale. In the RGB model, when $R = G = B$, this color represents a grayscale, and this value is the grayscale value of the image. In a grayscale, only one byte is needed for each pixel to store the gray value. The gray value range is 0-256. The commonly used image graying method:

$$r = g = nb = \frac{R + G + B}{3} \tag{1}$$

where R, G, and B are the three primary color values of the original image pixels and r, g, and b – the pixel value of grayscale after graying.

According to relevant literature, the conversion of color image to grayscale is not a simple calculation of the average of three color values, but follows the following calculation principles, which is actually an uneven distribution of energy:

$$r = g = nb = \frac{0.3008R + 0.5859G + 0.1133B}{3} \tag{2}$$

Image threshold segmentation and information feature discrimination: The basic idea of threshold segmentation is to use the difference between the grayscale values of the target and the background or between the grayscale values of the target and the target, take one or several appropriate grayscale values as the limit, and divide the image into two or more categories based on the threshold, so as to separate the target from the background or the target from the target.

Experiments

Construction of experimental platform

In order to test the effectiveness of the air source heat pump defrosting control method, an experimental environment room was built, in which the air source heat pump defrosting control method was experimentally tested. The purpose of this experimental test is to determine the starting and stopping conditions of defrosting control through experimental testing, in order to further test the feasibility and effectiveness of the air source heat pump defrosting control method based on image processing technology, and lay a foundation for further research in the future. Based on the aforementioned experimental objectives, an air source heat pump defrosting control system experimental platform was built and the system was debugged, and experimental testing was conducted on the heat pump unit [8].

This defrosting control system experiment was conducted in an experimental environment room, mainly including a heat pump unit, an experimental environment room, an air temperature and humidity regulation system, an image and data acquisition and control system*, etc.*

Heat pump unit. This test model is modified from the KFRd-36NW model of split ventilation. The air conditioner uses R22 as refrigerant and uses a slow moving air compressor. Heating capacity is 4050 W, cooling capacity is 3650 W, heating capacity is 1355 W, cooling capacity is 1350 W. The external heating of the heat pump is an *L*-type multi-circuit heating, and the external fan is an axial flow fan with an air volume of 1850 mph. The internal fan is a cross-flow fan with an air volume of 560 mph. Table 2 shows the standard structure of external electrical equipment.

Table 2. Structural parameters of outdoor heat exchanger

Size	Number of steel pipes	Pipe diameter	Pipe diameter distance	Fin type	Fin pitch	Fin thickness
755 mm × 23 mm × 550 mm	22	9.2 × 0.7 mm	25.2 mm	Plain film	1.4 mm	0.16 mm

Experimental testing and result analysis

Due to its simplicity and low cost, many manufacturers of air source heat pumps have favored the conventional temperature time defrosting control method. This strategy just has to gather the wall temperature at the gulf of the outside heat exchanger, and joined with the assurance of working time, the sensible control of thawing out can be acquired. Notwithstanding, frequently throughout the colder time of year activity of the intensity siphon unit, because of the constant changes in temperature and dampness of the outside air, this strategy frequently brings about *misleading thawing out*, which is frequently appeared as *awkward thawing out* and *thawing out without ice*, which truly influences the functioning productivity of the intensity siphon unit. To more readily grasp the powerful attributes of the testing unit during activity and thawing out, nearby testing was first directed on the adequacy of the first customary control thawing out arrangement of the unit.

Control logic of conventional temperature time defrosting control method:

Conditions for controlling the start of defrosting: Place the temperature testing probe on the inlet pipe wall of the outdoor heat exchanger, and test the temperature, t_w, of the pipe wall at the inlet of the heat exchanger. When the unit starts operating, start the measurement of the pipe wall temperature t_w. When t_w is less than or equal to 3 °C, start the time timer to record time, t. When the time timer accumulates to the set time and t_w is less than or equal to –3 °C, the unit meets the defrosting requirements and begins defrosting.

Conditions for controlling the end of defrosting: Continue to measure the wall temperature of the heating pipe while the device is in the defrosting position. When the temperature reaches or exceeds the temperature value, the unit meets the defrost end requirement, stops defrosting and enters the heating system. Actual tests were carried out in a test environment according to the reasons for air temperature control during the defrosting control method mentioned previously. Note that the two phenomena *no defrost time* and *dripless defrost* usually occur in outdoor climates with high temperatures and relative humidity that cause dew, and outdoor climates with low temperatures and relative humidity. Due to frequent occurrence of dew, two *fake thaw* experiments were carried out under cloud air temperature –6~0 °C, relative humidity 86~92, air temperature –12~6 °C, RH 60~70, RH, respectively:

The phenomenon of delayed defrosting: The phenomenon of *timed defrost* of air source heat pumps often occurs during operation of the device. The degree of air formation in the fins is already very large, which blocks the ventilation of the heater, thereby affecting the heat transfer of the evaporator, leading to sharp fluctuations in the temperature of the evaporator, which greatly affects the heating function of the unit, not defrosting in time can cause the device to block or break. The field evaluation of the phenomenon of *no defrosting time* was carried out in an experiment with an air temperature of –6~0 °C and a RH of 86~92. From the experiment, figs. 3 and 4 show the difference between the outside temperature and the inlet and fire temperature curves of the outdoor heater, respectively. As shown in fig. 3, when the room starts to work stably, the temperature of the external heat source decreases, and the temperature rises for 35 minutes, and the temperature of the external heating system continues, –7.4 °C, the

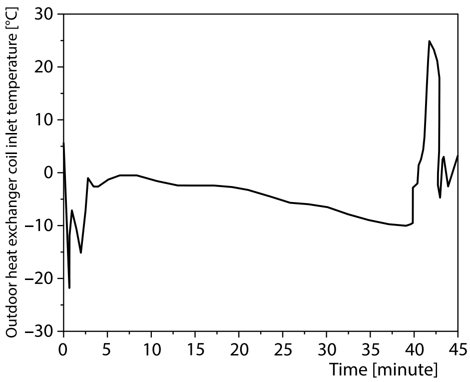

Figure 3. Change in inlet temperature of outdoor heat exchanger coil

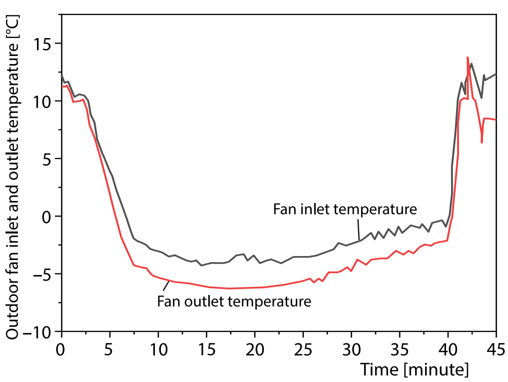

Figure 4. Changes in inlet and outlet temperature of outdoor fan

degree of decline gradually increased. When the heating time reaches 45 minutes, the inlet temperature of the external heating battery reaches –9.7 °C, at this point the room's defrosting point is reached, and the device starts defrosting. Those. It can be seen in fig. 4 that the temperature difference gradually decreases until the temperature difference between the input and output of the outdoor fan reaches 0.8 °C when the room operates for 45 minutes. It can be seen here that the drop layer blocks the fins of the heater and affects its heat transfer performance.

Determination of frost degree coefficient on the surface of outdoor heat exchanger fins

Based on the aforementioned defrosting process, the frost degree coefficient, *P*, on the surface of the fins can be calculated, and the values of each parameter in the formula are shown in tab. 3.

Table 3. Values of *p*-value calculation formula

Parameter	K_1	K_2	K_3	K_1	K_2
Value	0	0.6	2	85	210

Figure 5 shows the air cooling coefficient, *R*, on the surface of outdoor heating fins during defrosting. When the room begins to defrost, it can be seen that the freezing degree coefficient on the surface of the fins is observed depending on the thickness of the layer. When the defrosting process lasts 125 seconds, the freezing degree coefficient on the surface of the fin will decrease to 0.09 at this time. This is because during the first 125 seconds of defrost, the unit runs the compressor to reverse defrost, and the outside heat acts as a condenser. The temperature of the heating battery suddenly rises, and the layer quickly falls into the water and flows out, so the cooling coefficient of the air on the surface of the thermal fin decreases as the droplet decreases, indicating that it was a droplet, just melting all the while. After 120 seconds after defrosting, the unit's compressor turns off and the external fan turns on. The residual water on the surface of the fin is gradually evaporated by the residual heat of the coil and the action of the fan, until the water is completely gone, and during this process, the coefficient of the drop on the external heat surface to heat the fin. The *R* value remains at a low level of around 0.04. The entire defrosting process lasts 290 seconds, after which the heat pump resumes its heating operation [9, 10].

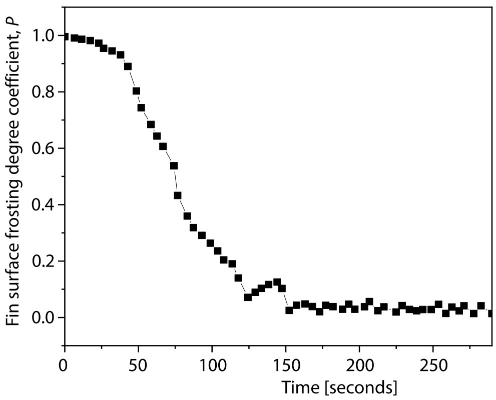

Figure 5. Frost degree coefficient on the surface of outdoor heat exchanger fins *P* changes in values

From the aforementioned defrosting process, it can be seen that the frost degree coefficient on the surface of the outdoor heat exchanger fins during the entire defrosting process *p*-value gradually decreases as the frost layer melts, until it remains at a lower level after defrosting is completed. Therefore, the *p*-value can intuitively reflect the changes in frost degree and can be used as an effective parameter to evaluate the changes in frost degree of outdoor heat exchangers. Utilize *p*-value, as the judgment value for defrosting start and stop, can truly reflect the frosting situation of the outdoor heat exchanger, it can improve the reliability of judgment and effectively prevent the occurrence of *false defrosting* phenomenon.

Conclusion

The author analyzes the development and research of the defrosting problem of air source heat pumps, explains the process of formation and growth of droplet layer on the water surface, based on a simple model according to the theory of heat and mass transfer. Create a mathematical model of cells, fins and layers on the surface of the fin, derive the heat balance equation for each body, separate and solve the equation. According to the image processing technology, a defrosting control method with an air source heat pump was proposed, and the defrosting control system was tested. thawing process.

Acknowledgment

This work was supported by the cultivation project for applying for master's degree programs of Leshan Normal University(2023SSDX005), and Leshan Normal University high level talents research start project(RC202038),and the key project of Leshan Science and Technology Bureau (20GZD024).

References

[1] Hao, Y., *et al*., Methods of Image Recognition of Overhead Power Line Insulators and Ice Types Based on Deep Weakly-Supervised and Transfer Learning, *IET Generation, Transmission and Distribution*, *41* (2022), 11, 16
[2] Aref Rajabi, *et al*., Optimization of Conjugate Heat Transfer in the Electrofusion Joint Using Taguchi Method, *Thermal Science*, *23* (2019), 5B, pp. 3047-3057
[3] Yan, W., *et al.*, Research on Non-Linear Distorted Image Recognition Based on Artificial Neural Network Algorithm, *Journal of Interconnection Networks*, *22* (2022), Suppl. 06, S41
[4] Rangayya, R., *et al.*, An Enhanced Segmentation Technique and Improved Support Vector Machine Classifier for Facial Image Recognition, *International Journal of Intelligent Computing and Cybernetics*, *41* (2022), 2, 15
[5] Chen, M., *et al*., Learning to Focus: Cascaded Feature Matching Network for Few-Shot Image Recognition, *Science China Information Sciences*, *64* (2021), 92105
[6] Liu, X., *et al*., Research and Application of Image Recognition of Substation Inspection Robots Based on Edge Computing and Incremental Learning, Non-Linear Optics, *Quantum Optics*, *41* (2022), 1-2, 56
[7] Lee, S., *et al*., Uav Pilot Status Identification Algorithm Using Image Recognition and Biosignals, *Journal of Advances in Information Technology*, *74* (2022), 5, 13
[8] Wei, C., *et al*., Development of a New Silicate Thermal Insulation Coating and Analysis of Heat Storage Characteristics, *Thermal Science*, *27* (2023), 2A, pp. 949-957
[9] Feng, J., *et al*., Research on the Application of Image Recognition Technology in Transformer Equipment Fault Monitoring, Non-Linear Optics, *Quantum Optics*, *41* (2022), 1-2, 56
[10] Guo, B., Friction Heat Energy Recovery System Based on Hydraulic Brake System by Wire of Heavy Vehicle, *Thermal Science*, *27* (2023), 2A, pp. 1159-1166

Paper submitted: June 26, 2023
Paper revised: August 24, 2023
Paper accepted: September 28, 2023